Available online at www.sciencedirect.com
SCIENCE DIRECT®
Journal of Solid State Chemistry 178 (2005) 8–14
JOURNAL OF SOLID STATE CHEMISTRY
www.elsevier.com/locate/jssc

Compressibility anomaly and amorphization in the anisotropic negative thermal expansion material $NbOPO_4$ under pressure

G.D. Mukherjee[a,*], V. Vijaykumar[a], A.S. Karandikar[a], B.K. Godwal[a], S.N. Achary[b], A.K. Tyagi[b], A. Lausi[c], E. Busetto[c]

[a]*High Pressure Physics Division, Bhabha Atomic Research Center, Mumbai, 400085, India*
[b]*Applied Chemistry Division, Bhabha Atomic Research Center, Mumbai, 400085, India*
[c]*ELETTRA, Sincrotrone Trieste, Trieste, Italy*

Received 12 August 2004; accepted 14 September 2004

Abstract

We report the results of the high-pressure angle dispersive powder X-ray diffraction measurements obtained up to 31 GPa on the monoclinic and the tetragonal phases of $NbOPO_4$. The tetrgonal phase was obtained by quenching the monoclinic phase from 5 GPa and 833 K. The lattice parameters of the monoclinic phase show an anomaly at 0.6 GPa, but the unit cell volume follow an almost linear compressional behavior. The bulk modulus B_0 and its pressure derivative B_0' are estimated to be 66(3) GPa and 1.6(8), respectively, for the monoclinic phase. The irreversible pressure induced amorphization observed at ambient temperature in the monoclinic phase is due to the kinetic hindrance to bond reconstruction that is required for transformation form the monoclinic to the tetragonal phase. In the case of tetragonal $NbOPO_4$, the compression is found to be anisotropic.

PACS: 62.50.+p; 07.3k.+k; 61.50.Ks; 61.10.Nz; 41.60.Ap

Keywords: High pressure; Pressure induced amorphization; Phase transition; NTE

1. Introduction

In recent years there have been considerable research interest [1] in materials with MO_2 [2], AM_2O_8 [3–5], AM_2O_7 [4,6,7], $A_2M_3O_{12}$ [4,8] and AMO_5 [9,10] stoichiometry (A and M are octahedral and tetrahedral cations, respectively) due to their structural flexibility to exhibit negative thermal expansion behavior (NTE). In the above materials the adjacent or the opposite corners of one octahedra link with the neighboring polyhedra by sharing the corner oxygen atom to form a three dimensional open network structure. Under pressure, the reduction in volume in these materials may lead to close-packed structures with linkages that favor denser phases (opposite corner or face-sharing polyhedra) or to structures with deformed polyhedra. Also amorphization may result if thermal activation to establish the new linkages is not available. Thus NTE materials are predisposed to display interesting behavior at high pressures. Also such ceramic materials that exhibit NTE are of technological importance because of the possibility to tune the thermal expansion of NTE-normal material composites [11]. During the preparation and the applications, local pressures inside the composites may change which may affect the phase stability of these NTE materials and hence a detail map of high pressure behavior of the NTE materials have become necessary for all practical purposes.

High pressure investigations on AM_2O_8 and $R_2M_3O_{12}$ (A = Zr, Hf; M = W, Mo, V; R = Sc, Lu, Ho) type NTE materials have revealed the existence of a

*Corresponding author. Fax: +91 22 2550 5151.
E-mail address: gdm@apsara.barc.ernet.in (G.D. Mukherjee).

0022-4596/$ - see front matter © 2004 Elsevier Inc. All rights reserved.
doi:10.1016/j.jssc.2004.09.011

number of structural transitions and amorphization, both reversible and irreversible [12–17]. The pressure induced amorphization in many of the above materials is attributed to the kinetic hindrance for formation of new phases. This has been demonstrated by the fact that ZrW_2O_8 transforms to a new dense hexagonal U_3O_8 type polymorph when heated under pressure just above the completion of the pressure induced amorphization [18]. Also the trigonal $HfMO_2O_8$ has been found to transform to a new monoclinic phase when quenched from high pressure and high temperature [19].

In our effort to study the high pressure behavior on NTE materials with AMO_5 stoichiometry, we selected $NbOPO_4$, which belongs to an unexplored subgroup of materials that exhibit anisotropic NTE [10]. At ambient conditions $NbOPO_4$ can be synthesized in a monoclinic phase (SG: $P2_1/c$) [10,20] or in a 18% denser tetragonal phase (SG: $P4/n$) [9]. Both the phases of $NbOPO_4$ are based on NbO_6 octahedra and PO_4 tetrahedra, which share corners to form three dimensional framework structures (Fig. 1). Both the phases undergo reversible transitions to higher symmetry phases: monoclinic to an orthorhombic phase (S.G.: *Pnma*) at 565 K [10] and tetragonal to another tetragonal phase (S.G.: $P4/nmm$) at 473 K [9]. Even though monoclinic $NbOPO_4$ exhibits positive volume expansion, *a*-axis is found to decrease with increasing temperature up to the phase transition temperature, 565 K [10]. However after the transition to the orthorhombic phase, it exhibits NTE [10]. Anisotropic NTE is observed in tetragonal $NbOPO_4$ above 473 K (i.e., after the transition) with a contraction in *ab*-plane (but with a net positive volume expansion) with increase in temperature [9].

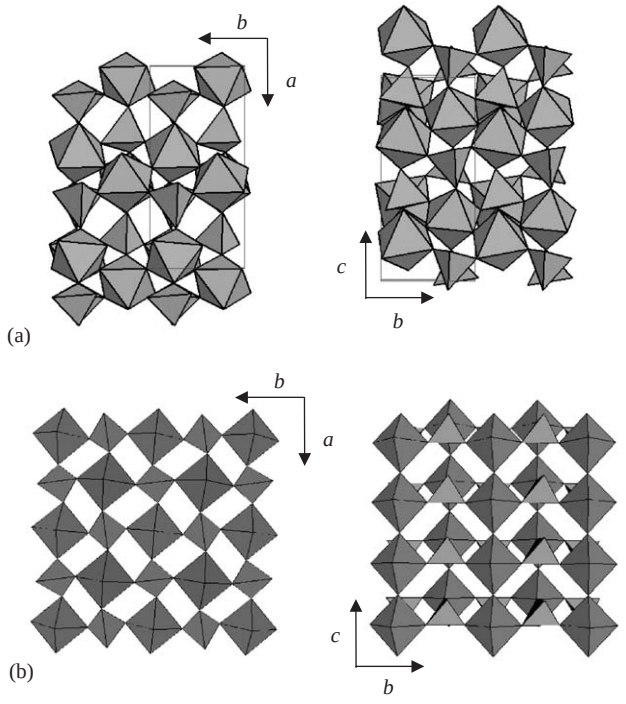

Fig. 1. Illustration of the structure of $NbOPO_4$ in its (a) monoclinic phase and (b) tetragonal phase.

In this article, we report the results of the structural investigations by in situ X-ray powder diffraction at high pressure on both the phases of $NbOPO_4$, which were carried out to explore the possibility of any pressure induced structural transition or amorphization.

2. Experimental

Monoclinic $NbOPO_4$ was synthesized by the reaction of Nb_2O_5 and phosphoric acid at 1573 K and then air quenching the sample [10]. Angle dispersive powder X-Ray diffraction (ADXRD) measurements were employed to characterize the material at ambient condition, and at high pressures. These measurements were carried out at the powder X-ray diffraction beam line of ELETTRA Synchrotron source, Trieste, Italy using monochromatized X-rays of wavelength 0.729 Å. For high pressure experiments fine powdered samples of $NbOPO_4$ were loaded in a Mao–Bell-type diamond anvil cell (DAC) [21]. A pair of diamond anvils with culet diameter of about 400 μm was used in the DAC. A hardened steel gasket with a central hole of diameter of 150 μm and thickness 60 μm contained the sample and the X-ray beam was collimated by 80 μm diameter pinhole. A mixture of methanol–ethanol (4:1) was used as pressure transmitting medium. The pressure was determined in situ by using Pt/Pd powder mixed with the sample as pressure calibrant within an estimated error of ±0.1 GPa. Images of the powder diffraction rings were collected with a Mar345 image plate detector and read with a resolution of 100 μm × 100 μm pixel size. Typical exposure times of 20–30 min were employed for measurements at high pressures. The images were integrated over the powder rings using the FIT2D software [22] and converted to the normal 2Θ vs. intensity diffraction pattern. The minimum *d*-spacing obtained from the high pressure experiment was 1.0657. The powder patterns so obtained were further corrected for the absorption by the diamond anvils. X-Ray powder patterns were collected up to 30 GPa. Since the monoclinic $NbOPO_4$ was found to amorphize gradually, it was subjected to high pressure and high temperature in a toroid anvil (TA) apparatus to investigate the presence of kinetically hindered phase transition, if any.

The TA is made up of a pair of tungsten-carbide anvils with face diameter 32 mm and cavity diameter 13.5 mm. The powdered sample, pressed into a cylindrical pellet of approximately 4 mm diameter and 5 mm length was encapsulated in a BN container and placed at the center of a graphite heater assembly, which forms the sample assembly. The sample assembly was then

enclosed in a pyrophyllite gasket, shaped to match the toroid anvil profile and was pressurized with a 400 ton press. The pressure–load calibration curve of the TA-apparatus was obtained using the Bi I–II and the Yb hcp to bcc transitions at 2.65 and 4 GPa, respectively. In the TA experiments, the pressure was initially raised slowly to 5.5 GPa and thereafter the temperature was increased to 833 K (i.e. well above the monoclinic to orthorhombic transition temperature) at the rate of about 10 K per minute. The pressurized sample was held at the final temperature and pressure for 15 min and then quenched by cutting off the heater electrical power. The sample was then retrieved after releasing the pressure and characterized by ADXRD measurements. All the X-ray lines observed in the retrieved sample were indexed to a tetragonal lattice. The structural evolution of this tetragonal phase with pressure was also investigated by X-ray powder diffraction at ELETTRA synchrotron source.

3. Results and discussion

3.1. Monoclinic $NbOPO_4$

The ambient pressure and room temperature ADXRD data on $NbOPO_4$ could be indexed to a monoclinic lattice with unit cell parameters: $a = 13.091(1)$ Å, $b = 5.279(2)$ Å, $c = 13.230(1)$ Å and $\beta = 120.615(4)^\circ$, in excellent agreement with literature values [20]. The reflection conditions for the indexed monoclinic phase indicate to the space group symmetry of $P2_1/c$ as mentioned in literature [10]. This choice of space group was further corroborated by the Rietveld refinement of the pattern using GSAS Rietveld refinement program [23] with the trial atom position parameters reported in literature [10].

Few typical X-ray powder patterns collected at high pressures and the pattern after pressure release are shown in Fig. 2. The evolutions of the ADXRD patterns with pressure show a gradual amorphization of monoclinic $NbOPO_4$ starting at 3.6 GPa. Gradually the sample lines broadened and merged with the background with increasing pressure. A careful inspection of the powder patterns show that with the application of pressure the line-broadening is initiated from the lines corresponding to low d (high 2Θ) values. No transition to another crystalline phase is observed up to the highest pressure of this study.

Since the monoclinic structure is too complex and the X-ray reflections broadended rapidly with increasing pressure, all high pressure ADXRD patterns were indexed and the Rietveld refinement was carried out on patterns up to 0.6 GPa with ambient atom positions parameters as starting values. Subsequently for all other high pressure ADXRD patterns profile fitting (Le Bail

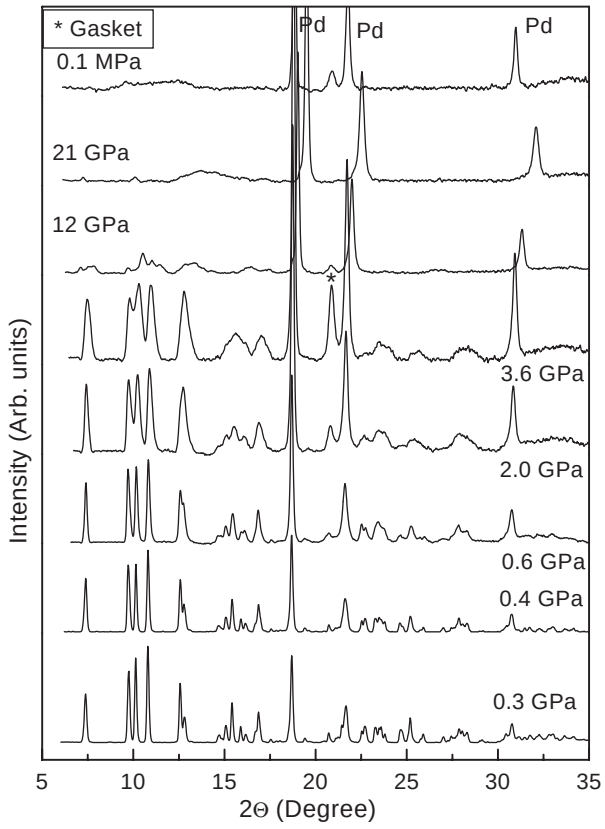

Fig. 2. Selected typical X-Ray powder patterns collected at high pressure and the pattern after pressure release (labeled as 0.1 MPa) with Pd as pressure calibrant.

method) was carried out using GSAS. Shifted Chebyshev background parameters and pseudo-Voigt profile parameters were employed for the fitting. A typical Rietveld refinement fit of the pattern obtained at 0.3 GPa is shown in Fig. 3, which yielded the values of residuals:

$$R_p \left(= \frac{\sum |y_i(\text{obs}) - y_i(\text{cal})|}{\sum y_i(\text{obs})} \right) = 0.026;$$

$$R_{wp} \left(= \left[\frac{\sum w_i [y_i(\text{obs}) - y_i(\text{cal})]^2}{\sum w_i [y_i(\text{obs})]^2} \right]^{(1/2)} \right) = 0.030$$

and

$$R_{F^2} \left(= \sum \frac{|F_{hkl}(\text{obs})^2 - F_{hkl}(\text{cal})^2|}{\sum F_{hkl}(\text{obs})^2} \right) = 0.22.$$

The behavior of the lattice parameters at various pressures up to 6 GPa is shown in Fig. 4. Above 6 GPa, indexing the powder patterns did not yield any meaningful result because of excessive broadening of the X-ray diffraction lines. However it may be noted that the diffraction lines from the pressure calibrant Pd are present and remained sharp. Therefore the broadening and disappearance of the lines are due to the pressure induced disorder in the lattice or the amorphization of

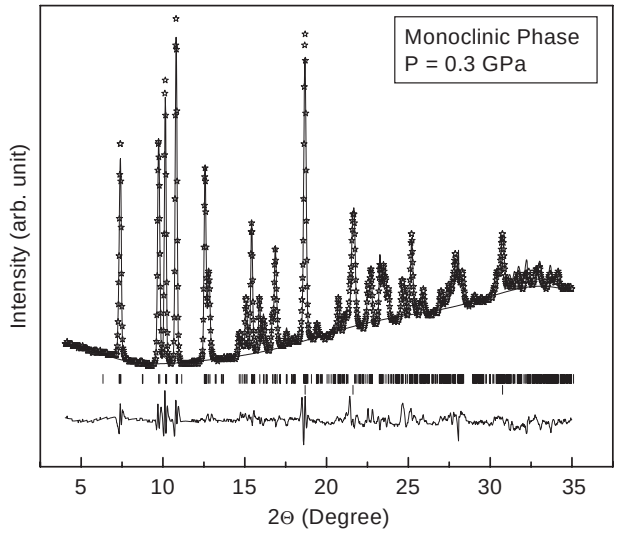

Fig. 3. Observed, calculated and difference plots for Rietveld refinements of monoclinic $NbOPO_4$ at 0.3 GPa.

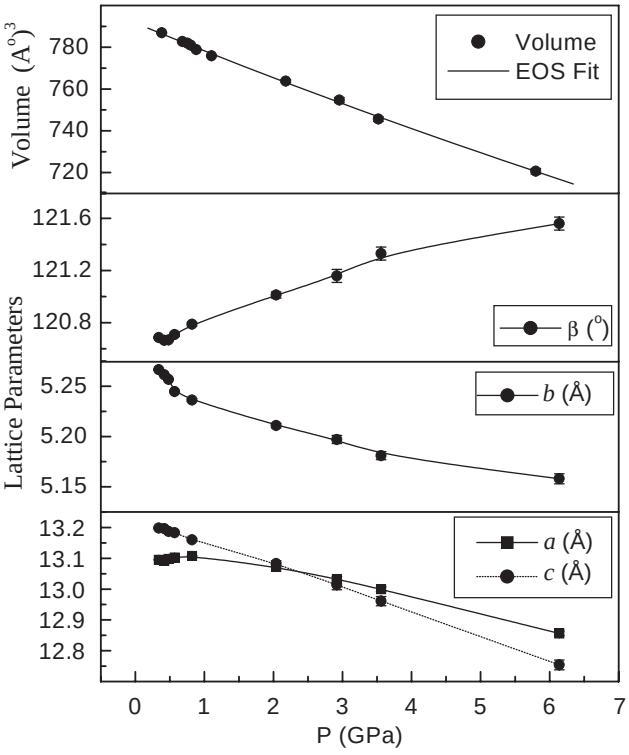

Fig. 4. Pressure evolution of the lattice parameters and the volumes of monoclinic $NbOPO_4$. The lines are just guide to the eye for the case of lattice parameters, whereas the solid line in volume represents the equation of state fit using the Birch–Murnaghan function.

the material. The lattice parameters (Fig. 4) show an anomaly at about 0.6 GPa with a slope change in *a*- and *b*-cell parameters. Also angle β starts increasing from 0.6 GPa. However the volume decreases linearly with pressure up to 6 GPa. The measured P vs. V data are fitted to the Birch–Murnaghan equation of state [24] using EOSFIT program [25]. The values of bulk modulus B_0 and its pressure derivative B_0' are estimated to be 66(3) GPa and 1.6(8), respectively. The low compressibility value and its pressure derivative indicates to a large continuous reduction (almost linear) in the volume of the material at high pressure. Such linear P vs. V relations are observed in several materials with small or negative thermal expansion [26].

As mentioned in the introduction, the crystal structure of monoclinic $NbOPO_4$ is based on NbO_6 octahedra and PO_4 tetrahedra, which share corners to form three-dimensional networks with large open spaces. The two adjacent corners of NbO_6 octahedra are used to form zigzag chains along the *b*-axis (Fig. 1). The results of Rietveld refinement showed that the average polyhedral linking angle Nb–O–P increased slightly from 159.4(6)° to 161.2(14)° by 0.6 GPa. The observed change in the polyhedral linking angles up to 0.6 GPa along with the initial large compression of *b*-axis is probably because of the rotation of NbO_6 polyhedra to reduce the length of the chains along this direction. This can accommodate the volume reduction in the material by partially filling up the open spaces.

It is interesting to note that under pressure, the monoclinic phase does not transform to the tetragonal phase even though it is 18% denser. Instead the material amorphizes at high pressures. The absence of sample lines in the ADXRD pattern of the pressure released sample (Fig. 2) shows that the pressure induced amorphization is irreversible. It may be noted that in the monoclinic phase the adjacent corners of the NbO_6 octahedra are linked to PO_4 tetrahedra where as in the tetragonal phase it is the opposite corners of the NbO_6 octahedra that are linked to the PO_4 tetrahedra. Thus it seems that the failure to reconstruct the new bonds in the absence of thermal activation leads to amorphization. The fact that monoclinic $NbOPO_4$ transforms to the 18% denser tetragonal phase at 5.5 GPa and 873 K is consistent with this conclusion.

3.2. Tetragonal $NbOPO_4$

The ambient X-ray lines of the quenched $NbOPO_4$ could be indexed to a tetragonal lattice with cell parameters: $a = 6.387(3)$ Å and $c = 4.097(2)$ Å with a unit cell volume of 167.17(20) Å^3. The c/a ratio of this phase is calculated to be 0.64, which is equal to the reported tetragonal phase of $NbOPO_4$ with space group $P4/n$. Therefore all the further analyses on quenched $NbOPO_4$ are carried out on the space group $P4/n$. The density of the tetragonal phase is found to be 18% higher than the parent monoclinic $NbOPO_4$.

The pressure evolution of this tetragonal phase was investigated up to 30 GPa. Few typical X-Ray powder patterns collected at high pressures and the pattern after

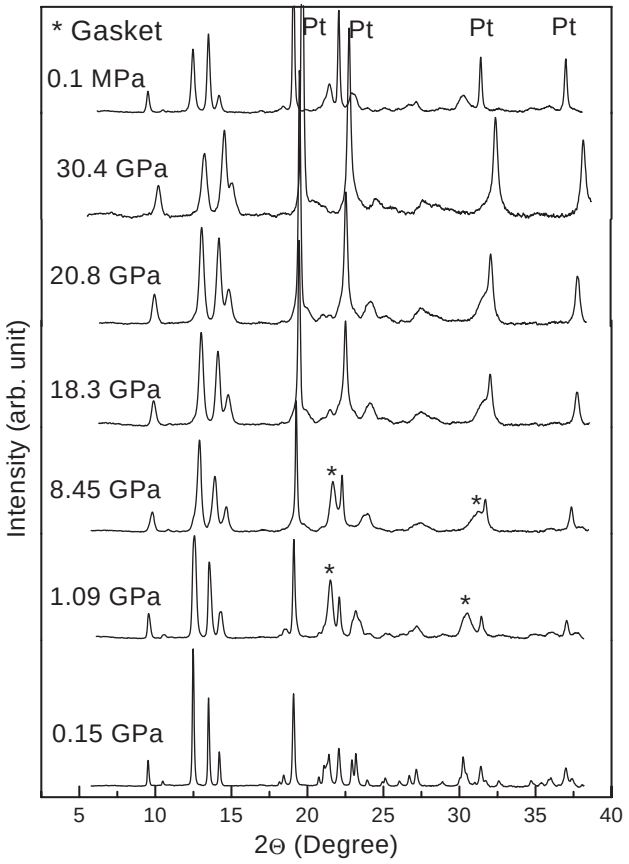

Fig. 5. Selected typical X-Ray powder patterns of tetragonal $NbOPO_4$ collected at high pressure and the pattern after pressure release (labeled as 0.1 MPa) with Pt as pressure calibrant.

pressure release are shown in Fig. 5. The evolution of the ADXRD patterns with pressure shows a slight broadening of X-ray lines, which is prominent at the low *d*-value region. The Rietveld refinement of the pattern obtained at 0.15 GPa was initiated using the atom positional parameters available in literature [9] along with the pseudo-Voigt profile function, scale parameters and the sixth background function as given in the GSAS program, which fits the background contributions that tend to rise at small *d*-values as seen in our ADXRD patterns. The final refinement produced fits with the typical values of residuals: $R_p = 0.032$, $R_{wp} = 0.050$ and $R_{F^2} = 0.255$. Results of the typical Rietveld refinement employing GSAS for the pattern at 0.15 GPa is shown in Fig. 6. For all other high pressure powder ADXRD patterns, Le Bail refinement (for refinement of non-structural parameters) was carried out using GSAS.

The pressure variation of lattice parameters and volumes are shown in Fig. 7. The *P* vs. *V* curve could not be fitted to any single equation of state function (EOS) in the whole pressure range (up to 30 GPa). An inspection of the *P* vs. *V* curve show a slope change at about 18 GPa. Therefore the cell volume is fitted up to 18 GPa using the Vinet EOS [27,28] and it yielded the

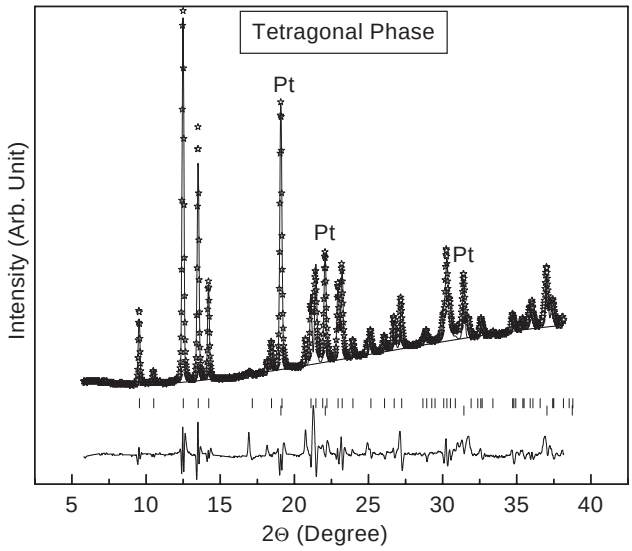

Fig. 6. Observed, calculated and difference plots for Rietveld refinements of tetragonal $NbOPO_4$ at 0.15 GPa.

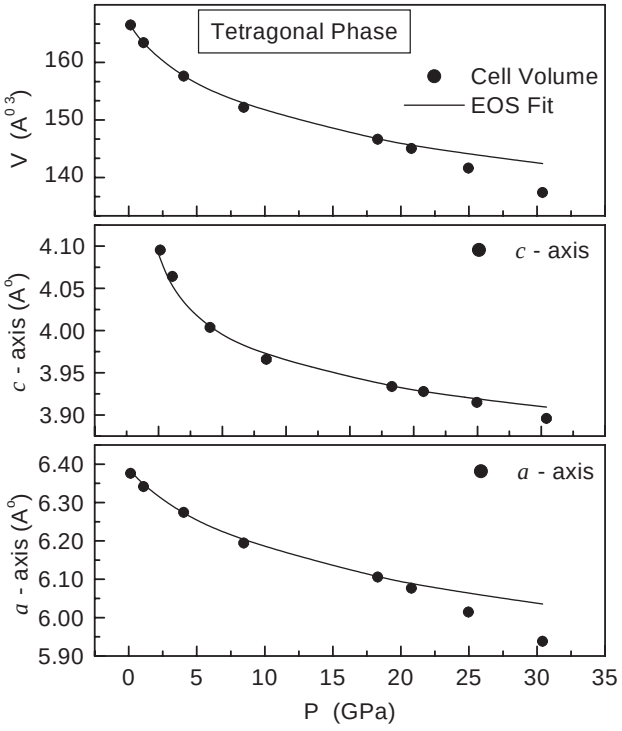

Fig. 7. Change in cell edges and cell volume of tetragonal $NbOPO_4$ with pressure. The solid lines drawn through *a*- and *c*-cell edge data points are guide to the eye.

values of the bulk modulus (B_0) and its pressure derivative (B_0') to be 34(2) GPa and 22.2(9), respectively. These values need to be confirmed with high pressure ADXRD measurements at close pressure intervals. However similar small B_0 and large B_0' are found to be characteristic for materials with strongly anisotropic compression properties such as α-NaV_2O_5 [29],

archetypical graphite [30], $CuGeO_3$ [31] and many superconductors [32]. In the low-pressure region, up to 8 GPa, the *c*-cell edge reduces by about 3.5%, where as the *a*-cell edge decreases by about 2.6%. Also the pressure variations of both the *a*- and *c*-cell edges show deviation above 18 and 25 GPa, respectively, from those extrapolated from the lower pressures (Fig. 7). The above behavior show an anisotropy in the compression of the tetragonal $NbOPO_4$.

In the tetragonal phase of $NbOPO_4$ two opposite corners of NbO_6 octahedra are linked to two lateral PO_4 tetrahedra to form linear chains along *a*/*b*-axis and the two opposite corners of NbO_6 octahedra are used to form linear chains along *c*-axis Fig. 1(b). The larger compression up to about 8 GPa along *c*-direction indicates to the compression as well as deformation of the larger NbO_6 polyhedra. The presence of large open spaces in the structure along with smaller anion–anion repulsion forces in the octahedra results in the deformation of larger NbO_6 octahedra.The slope change observed along *a* - edge above 18 GPa is probably due to the change in the linking angles of NbO_6 and PO_4 polyhedra.

The increase in compressibility above 20 GPa as evident from Fig. 7 can be due to the onset of disorder with increasing polyhedral deformation in the tetragonal phase of $NbOPO_4$, which is indicated in the broadening of the X-ray reflections as shown in Fig. 5. The presence of disorder induced is evident from the ADXRD pattern of the pressure released sample, where no sharp sample lines are seen at high angles. But no pressure induced amorphization is observed in the tetragonal phase up to 30 GPa, the highest pressure of this investigation. This is probably due to the fact that the tetragonal phase is 18% denser than its monoclinic counterpart, which prevents the movements of anions. Therefore the compression in the material takes place by polyhedral volume reduction, which is governed by the anion–anion repulsion forces and polyhedral deformation.

From the above discussions it is clear that the different compressional mechanisms observed in both the phases of $NbOPO_4$ are mainly due to their different connectivity of NbO_6 octahedra and PO_4 tetrahedra. In case of monoclinic phase the adjacent corners of the NbO_6 octahedra connect each other to form zigzag chains along *b-axis*. The octahedra and the tetrahedra connect each other to form a three dimensional spring like structure, which is more evident in the *bc* plane of the monoclinic phase of $NbOPO_4$ (Fig. 1(a)). This spring like behavior of the material is reflected in the almost linear pressure derivative of bulk modulus in the monoclinic phase. As shown in Fig. 1(b), in the case of tetragonal phase the connectivity of the structural elements leads to the formation of layers in the *bc* plane. Two nearest linear chains of octahedra are separated from each other by PO_4 tetrahedra leaving open spaces along *c-cell* edge. This probably results in the larger compressibility in the *c* direction leading to the observed anisotropic compression in the tetragonal phase.

4. Conclusion

We report the results of the high pressure ADXRD measurements carried out up to 31 GPa on the monoclinic and the tetragonal phases of $NbOPO_4$, where the later phase was obtained by quenching the monoclinic phase from 5 GPa and 883 K in a toroid anvil apparatus. The monoclinic phase undergoes gradual amorphization starting at about 3.6 GPa. The anomaly observed in the lattice parameters at 0.6 GPa is due to the rotation of the NbO_6 and PO_4 polyhedra at such low pressures. Almost linear compression in the monoclinic phase is attributed to the connectivity of the structural elements to form a spring type three dimensional network structure. Results from the high pressure and high temperature treatment of the monoclinic $NbOPO_4$ points to the kinetically hindered monoclinic to tetragonal phase transformation, which is responsible for the pressure induced amorphization of the monoclinic phase. No structural transitions including amorphization is observed in the tetragonal phase up to about 30 GPa pressure. There appears a pronounced non-linear compressional behavior in the tetragonal phase with the values of B_0 and B_0' estimated to be 34(2) GPa and 22.2(9), respectively. The large pressure derivative of bulk modulus is probably due to the anisotropic compression of the material and large deformation of the NbO_6 polyhedra.

Acknowledgments

The work has been carried out through the proposal no. 2002087 of ICTP-ELETTRA Users Program. GDM and VVK wishes to thank ICTP, Trieste, Italy for local hospitality and travel support for carrying out the experiments.

References

[1] A.W. Sleight, Inorg. Chem. 37 (1998) 2854 and the references therein.
[2] M.P. Attfield, A.W. Sleight, Chem. Commun. 601 (1998).
[3] J.S.O. Evans, T.A. Mary, T. Vogt, M.A. Subramanian, A.W. Sleight, Chem. Mater. 8 (1996) 2809.
[4] J.S.O. Evans, T.A. Mary, A.W. Sleight, J. Solid State Chem. 133 (1997) 580.
[5] J.S.O. Evans, T.A. Mary, T. Vogt, A.W. Sleight, Science 272 (1996) 90.
[6] V. Korthuis, N. Khosrovani, A.W. Sleight, N. Roberts, R. Dupree, W.W. Wareen Jr., Chem. Mater. 7 (1995) 412.

[7] J.S.O. Evans, T.A. Mary, A.W. Sleight, J. Solid State Chem. 137 (1998) 148.
[8] J.S.O. Evans, T.A. Mary, A.W. Sleight, Physica B 241 (1998) 311.
[9] T.G. Amos, A. Yokochi, A.W. Sleight, J. Solid State Chem. 141 (1998) 303.
[10] T.G. Amos, A.W. Sleight, J. Solid State Chem. 160 (2001) 230.
[11] H. Holzer, D.C. Dunand, J. Mater. Res. 14 (1999) 780.
[12] H. Liu, R.A. Secco, M. Imanaka, G. Adachi, Solid State Commun. 121 (2002) 177 and references therein.
[13] D.V.S. Muthu, B. Chen, J.M. Wrobel, A.H.K. Anderson, S. Carlson, M.B. Kruger, Phys. Rev. B 65 (2002) 064101.
[14] B. Chen, D.V.S. Muthu, Z.X. Liu, A.W. Sleight, M.B. Kruger, Phys. Rev. B 64 (2001) 214111.
[15] H. Liu, R.A. Secco, N. Imanaka, G. Adachi, Solid State Commun. 121 (2002) 177 and references therein.
[16] J.S.O. Evans, Z. Hu, J.D. Jorgensen, D.N. Argyriou, S. Short, A.W. Sleight, Science 275 (1997) 61.
[17] C.A. Perottoni, J.A.H. da Jornada, Science 280 (1998) 886.
[18] A. Grzechnik, W.A. Crichton, K. Syassen, P. Adler, M. Mezouar, Chem. Mater. 13 (2001) 4255.
[19] S.N. Achary, G.D. Mukherjee, A.K. Tyagi, B.K. Godwal, Phys. Rev. B 66 (2002) 184106.
[20] A. LeClaire, H. Chahboun, D. Groult, B. Raveau, Z. Kristallogr. 177 (1986) 277.
[21] V. Vijaykumar, S. Meenakshi, BARC Technical Report, LISD, BARC, Mumbai, August, 2000.
[22] A. Hammersley, FIT2D V10.3 Reference manual V4.0 ESRF, Grenoble, France, 1998.
[23] A.C. Larson, R.B. von Dreele, LANCE, Los Alamos National Laboratory, Los Alamos, NM, 1994;
W.A. Dollase, J. Appl. Crystallogr. 19 (1986) 267.
[24] F. Birch, Phys. Rev. 71 (1947) 809.
[25] R.J. Angel, Ed.R.M. Hazen, Comparative crystal chemistry, MSA Rev. Mineral. 39 (2000).
[26] S.K. Sikka, J. Phys.: Condens. Matter 16 (2004) 1033.
[27] P. Vinet, J. Ferante, J.R. Smith, J.H. Rose, Phys. C: Solid State 19 (1986) L467.
[28] P. Vinet, J. Ferante, J.H. Rose, J.R. Smith, J. Geophys. Res. 92 (1987) 9319.
[29] I. Loa, K. Syassen, R.K. Kremer, U. Schwarz, M. Hanfland, Phys. Rev. B 60 (1999) 6945.
[30] M. Hanfland, H. Beister, K. Syassen, Phys. Rev. B 39 (1989) 12598.
[31] S. Bräuninger, U. Schwarz, M. Hanfland, T. Zhou, R.K. Kremmer, K. Syassen, Phys. Rev. B 56 (1997) 11357.
[32] C. Fanggao, M. Cankurtaran, G.A. Saunders, A. Al-hffaji, D.P. Almond, P.J. Ford, Supercond. Sci. Technol. 4 (1991) 13.